

1969

Cracked beam test, May 1969

P. Marek

M. Perlman

A. W. Pense

L. Tall

Follow this and additional works at: <http://preserve.lehigh.edu/engr-civil-environmental-fritz-lab-reports>

Recommended Citation

Marek, P.; Perlman, M.; Pense, A. W.; and Tall, L., "Cracked beam test, May 1969" (1969). *Fritz Laboratory Reports*. Paper 2001.
<http://preserve.lehigh.edu/engr-civil-environmental-fritz-lab-reports/2001>

This Technical Report is brought to you for free and open access by the Civil and Environmental Engineering at Lehigh Preserve. It has been accepted for inclusion in Fritz Laboratory Reports by an authorized administrator of Lehigh Preserve. For more information, please contact preserve@lehigh.edu.

Low-Cycle Fatigue

CRACKED BEAM TEST

by

P. Marek

M. Perlman

A. W. Pense

L. Tall

This work was conducted as part of a study of low-cycle fatigue, sponsored by the Office of Naval Research, Department of Defense, under Contract N 00014-68-A-514; NR 064-509. Reproduction in whole or part is permitted for any purpose of the United States Government.

Department of Civil Engineering
Department of Metallurgy and Materials Science

Fritz Engineering Laboratory
Lehigh University
Bethlehem, Pennsylvania

May, 1969

Fritz Engineering Laboratory Report No. 358.4

TABLE OF CONTENTS

	<u>Page</u>
ABSTRACT	i
1. INTRODUCTION	1
2. DESCRIPTION OF THE TEST	4
1. Specimen	4
2. Instrumentation	4
3. Test Program and Recording	5
4. Metallographic Examination	7
3. TEST RESULTS	8
1. Crack Propagation and Strain Recording	8
2. Metallographic Results	9
4. DISCUSSION	10
1. Crack Initiation	10
2. Residual Stresses	10
3. Crack Propagation Rate	10
4. Stress Redistribution	13
5. Metallographic Studies	14
Structure and Properties of Plate	14
High-Cycle Fatigue Crack	16
Low-Cycle Fatigue Crack	17
Web and Flange Crack Ends	17

TABLE OF CONTENTS - CONTINUED

	<u>Page</u>
5. CONCLUSIONS	19
6. NOMENCLATURE	22
7. ACKNOWLEDGEMENTS	23
8. TABLES AND FIGURES	25
9. REFERENCES	46

ABSTRACT

This report presents the results of and discussion on an experimental investigation of a welded beam with a crack tested in the low-cycle fatigue range.

In the investigation, an attempt was made to develop techniques for evaluating low-cycle tests. The tests conducted were designed for different kinds of measurements for beam tests, to gain experience with data recording, to obtain preliminary information about crack propagation, to try to record stress redistribution, and to obtain information on the metallurgical structure sensitivity of low-cycle and high-cycle fatigue tests.

The test was conducted on a beam already cracked in a high-cycle fatigue test. The relationship between the crack propagation rate, stress redistribution and the texture of the crack surface were observed. The recorded data were compared with available theoretical or experimental results.

1. INTRODUCTION

Design for low-cycle fatigue resistance requires an approach different from that of high-cycle fatigue. In high-cycle fatigue, the stresses remain generally in the elastic range except for a very small zone of plastic strain at the leading edge of the crack. In low-cycle fatigue, the cyclic strains promoting development and extension of cracks are functions of stress redistribution and geometry of the component in terms of a plasticity analysis. To obtain the necessary information about the stress-strain conditions in the section, and especially at the crack tip zone, and also about the cycling stress-strain history of each fiber, the stress redistribution process in highly stressed components needs to be investigated.

In this investigation an attempt was made to develop analytical and experimental techniques for evaluation of low-cycle tests. The tests conducted were designed:

- a) to try different kinds of measurements for low-cycle fatigue testing on beams
- b) to get experience with recording
- c) to get pilot information about crack propagation in the tension flange and its recording

- d) to try to record the stress redistribution in the flange and the web
- e) to obtain preliminary information on the metallographic structure sensitivity of low-cycle and high-cycle fatigue tests.

The test is not typical of low-cycle fatigue investigations, since it is actually the second part of a beam fatigue test. With respect to the purpose of this study, to obtain information about stress and strain observations in the range of high yielding, this beam has certain advantages. These are:

- the crack initiation had already occurred and thus crack propagation could be readily observed and monitored
- comparisons of high and low cycle crack growth morphology could be made in one specimen
- material and fatigue history in the high-cycle fatigue tests were known and documented
- the presence of a preexisting complex crack shape (3 ended) presented an interesting experimental and analytical problems for study
- the residual stress patterns in this beam were well documented
- the fact that the beam was welded, allowed analysis of the influence of welding on fatigue behavior

- low cycle fatigue test results on tensile coupons of the same material were available to assist in the analysis of the data.

Since the test was actually a composite one, containing both low-cycle and high-cycle fatigue portions, the expression "low-cycle fatigue" will be used for the second portion and "high-cycle fatigue" for the initial portion of the test.

2. DESCRIPTION OF THE TEST

2.1 Specimen

The cracked welded beam marked PWC152-A514 which had been used already in a high-cycle fatigue investigation⁽¹⁾ was tested after its length had been altered to suit the testing machine and after some small cracks in the web and the flange away from the investigated section had been repaired. The cross-section and the position of the cracks are shown in Fig. 1. The original crack was obtained in the tension flange after 397,000 cycles of high-cycle fatigue testing, where the stress range in flanges was 42 ksi and the maximum nominal stress + 32 ksi. The original crack shape is presented in Figs. 1 and 2.

The alternating load in the second phase of the fatigue test (the "low-cycle fatigue") was $L_1 = 80$ kips and $L_2 = 30$ kips, where L_1 and L_2 define the load bounds of the range. This loading should result in a nominal maximum stress of 36.2 ksi and a stress range of 22.6 ksi in the flanges (virgin section).

2.2 Instrumentation

Crack propagation, strains and deflections were measured

and recorded during the fatigue test. The following instrumentation was used in the testing:

- a) strain gages (marked 1, 2, 10, 20, 3, 4, 5 in Figs. 2 and 3).
- b) the static strains were recorded using a Budd Datran Digital Strain Indicator and the cyclic strains were recorded using a Brush Recorder and an Oscilloscope
- c) crack propagation gages (marked a, b, c, d) in Fig. 2. The propagation was recorded by the Brush recorder
- d) a microscope was used for visual crack propagation readings
- e) a dial gage was used for measuring deflection of the beam.

2.3 Test Program and Recording

The loading of the beam in the low cycle fatigue test was started by static loading to the maximum load $L_1 = 80$ kips while all recording channels were checked. The first set of strain gage readings were taken for different loads starting from zero kips up to 80 kips. The vertical deflection for load L_1 was recorded.

The dynamic test was conducted in phases based on 5000 cycles of alternating load. The minimum load was 30 kips and the maximum load was 80 kips. The Amsler machine was operated at 250 cycles per minute. The maximum dynamic load was adjusted slightly to get the same deflection as was recorded for static load. After each phase, the strains were recorded under static loads of 80 kips and zero kips. Static readings are missing for the 15000 and the 20000 cycles phases, when the strain gages were being connected to the Brush recorder (6 channels). Results with the Brush recorder gave a lower accuracy, and for further readings the Budd Datran Digital strain indicator was used again.

Crack propagation was recorded by crack propagation gages and observed visually by microscope.

The crack propagation gages connected to the Brush recorder gave very exact information about the crack propagation rate, but only within the interval of gage width.

Satisfactory visual recordings by the microscope were made. However there were some difficulties in following the crack tip at the beginning when it was short. Even under an 80 kip static load the crack was not open enough to make the tip position very clear. Later in the test it was possible to follow the crack tip while cycling with very good accuracy. The two main difficulties involved when using the microscope were: the lack of suitable reference lines against which to make visual readings and the

impossibility of visually recording crack propagation on the bottom side of the flange.

The deflection dial gage was used only to adjust dynamic load to correspond with static load. Deflection was not recorded.

The crack opening was measured but only in the last phase of test for both maximum and minimum static load.

2.4 Metallographic Examination

At the conclusion of the low-cycle test the failed beam sections were made available for metallographic examination. The tension flange and adjacent web were sectioned as shown on Fig. 4. Since the beam was welded from ASTM A514J steel which is quenched and tempered, all sectioning was done by saw cutting with lubricant to avoid any heat affects due to the sectioning procedure.

Photographs of the beam as sectioning proceeded are shown in Fig. 5.

These specimens were polished by standard metallographic procedures and were examined and photographed before and after etching.

3. TEST RESULTS

3.1 Crack Propagation and Strain Recording

After comparison of visual records with records from crack propagation gages, the shape of crack (Fig. 2) and the relationship between the number of cycles and crack length (Fig. 6) was obtained. For the flange half marked W, Fig. 6 shows the information available about the crack propagation on both the top and bottom surfaces separately and also an average value curve. In the range from zero to 37000 cycles the crack propagation rate was almost constant, then it increased gradually to a very high value before failure.

The strain gage readings are plotted in Figs. 7, 8, and 9. The top curves correspond to elastic strain due to static loads of 80 kips, and the bottom curves are assumed to correspond with the gradually developed and/or redistributed residual stress at 0 kips load.

The recording of crack propagation in the web was not satisfactory. Therefore only a little information is available. It includes the initial crack length, the final crack length and the number of cycles when the crack tip reached strain gage No. 3. The assumed crack propagation is shown in Fig. 10. The final crack

length includes an increment, Δcr , (Fig. 10) probably caused by impact when the flange failed. The description of the crack tip region is included in the next chapter.

The strain gage readings in the web are plotted in Fig. 10 and the stress redistribution is estimated by assuming the yield stress and gradually increasing plastic zone at the crack tip.

3.2 Metallographic Results

The fracture surfaces were examined macroscopically to characterize the nature (rough, delaminated, smooth) and orientation of the fracture to the test beam (see Fig. 5). After sectioning and polishing, see Fig. 4, the specimens were examined as-polished and after a Nital etch.

Figure 11 is a section normal to the flange crack in a region of the crack formed in high-cycle testing. Figure 12 is a section normal to the flange crack near the outside of the flange (low-cycle test range).

The ends of the web and flange crack (see Figs. 4 and 5) are shown in Figs. 13 and 14.

4. DISCUSSION

4.1 Crack Initiation

The high-cycle fatigue testing and crack initiation studies on the beam are discussed in Ref. 1. In beam PWC 152 the crack initiated at a tack weld end as shown in Fig. 15 and was growing very slowly through the flange-to-web welds, the central part of the flange, and the top of the web. The crack was observed after only 386,300 cycles.

4.2 Residual Stresses

Similar weld shapes were investigated to obtain information about residual stresses in the virgin beam and the stress redistribution after loading.⁽²⁾ The average residual stress pattern for the beam PWC 152 is shown in Fig. 16.

4.3 Crack Propagation Rate

For the high-cycle test, there is no record of the crack propagation. However the first observation of the crack, the final

crack length and increase in beam deflection in the last stage of high-cycle fatigue test were recorded.⁽¹⁾

The crack length versus the number of cycles for the low-cycle fatigue test is shown in Fig. 6. The rate of crack propagation $\frac{d(2a)}{dN}$ versus nondimensional ratio $\frac{2a}{w}$ is plotted in Fig. 17, where $2a$ is the total length of the crack, N - number of cycles and w - width of the flange.

In Fig. 17 theoretical values are also shown for both high- and low-cycle fatigue tests of crack propagation rate versus $\left(\frac{2a}{w}\right)$ to allow comparison with the measured values.

The theoretical curves were obtained assuming:

1. yield stress $\sigma_{ys} = 110$ ksi

2. $\Delta k = \Delta \sigma \sqrt{\pi a \sec \frac{(a + r_y)}{W}}$ and

$$r_y = \frac{1}{2} \pi \left(\frac{\Delta k}{\sigma_{ys}} \right)^2 \quad (\text{see Ref. 3})$$

valid for a plate of finite width

3. $\Delta \sigma$ = stress range (different for high- and low-cycle fatigue phase)

4. relationship Δk versus $\left(\frac{da}{dN}\right)$ for A514 with correction for high Δk , from Ref. 3

5. residual stress, the three-end crack behavior, and the corresponding stress redistribution are all neglected.

Assuming the theoretical relationship between $\frac{d(2a)}{dN}$ and $\frac{2a}{w}$ for the high-cycle fatigue test in Fig. 17 is a straight line, the crack propagation rate is

$$\frac{d(2a)}{dN} = \frac{6 \times 10^{-5}}{1.55} \cdot X$$

where X is equal to crack length. The number of cycles required to extend the crack length from value $2a$ to $1.55''$ may be obtained from

$$\int_{2a}^{1.55} \frac{dx}{X} = \frac{6 \cdot 10^{-5}}{1.55} \int_0^N dN$$

and

$$N = \frac{1.55}{6 \cdot 10^{-5}} [\lg X]_{2a}^{1.55}$$

The values of $2a$ for the low-cycle fatigue test were obtained in a similar way. The computed values are plotted in Fig. 18 for comparison with the values recorded in the low-cycle test.

The discontinuity of crack propagation rate in high- and low-cycle fatigue test (Fig. 17) is apparently caused mainly by the

decrease in stress range from high-cycle to low-cycle testing and the restraining effect of three-ended crack propagation. The recorded values of the crack propagation rate in the first phase of the low-cycle fatigue test are higher than the theoretical values, and the crack length (Fig. 18) coincides with recorded values only in the last phase of fatigue life. A possible explanation for the recorded behavior of the crack growth curve in the first phase of the low-cycle test may be that the region at the crack tip produced in the high-cycle tests, which has already seen a rather high level of Δk , undergoes fatigue damage. As a result, in the subsequent low-cycle tests, growth rates are higher than theoretically expected. However, this physical region of rapid crack growth is too large to attribute to fatigue damage alone. Therefore it appears that the residual stress pattern and the complex (three-ended) crack shape might also be of importance.

4.4 Stress Redistribution

The stress distribution in the cracked cross section as obtained from strain gage readings is shown for the web in Fig. 10 and for the flange in Fig. 19.

In the web, the assumed stress distribution curve is plotted through three recorded points and the yield stress zone at the crack tip as on plots. It was assumed also that the

plastic zone close to the crack tip is increasing with the crack propagation.

The stress distribution in the flange was first analyzed theoretically using the simplified mathematical model and computer program described in Ref. 4. The residual stress pattern (Fig. 16) was taken into consideration. The stress redistribution was obtained for some crack propagation stages also by the computer program. The stress distribution for $N = 0$ and loading $L_1 = 80$ kips was used as the reference curve and recorded stresses were plotted to get comparison of theoretical and recorded stresses. For strain gage No. 2 the results are coincident, but for strain gage No. 20 the theoretical values are slightly higher than the recorded data. This difference is caused mainly by simplification of the theoretical assumptions (such as simple plate, 3-ended crack neglected, uniaxial stress taken into consideration).

The behavior of the three-ended crack in a beam and the corresponding stress redistribution cannot be simulated by the behavior of a simple finite plate, and the theoretical analysis and mathematical model for this problem will be developed.

4.5 Metallographic Studies

Structure and Properties of Plate

The beam test was conducted on steel meeting the requirements of ASTM A514, Type J.⁽⁵⁾ This is a quenched and tempered

steel which is weldable and has a minimum yield strength of 100,000 psi and an ultimate strength of 115,000 to 135,000 psi. The mechanical properties of the material obtained by test are given in Ref. 1.

These properties are attained by heating to not less than 1650°F, water quenching and tempering at not less than 1100°F. Such a heat-treatment usually results in a tempered martensite microstructure.

In the case of A514 Type J, the only special alloying elements added are Mo and B. The hardenability (ability to quench to all martensite) is obtained through a severe cooling rate imposed by roller quenching. Tempering results in a complex and fine tempered martensite structure. This structure may be seen in Figs. 11, 12 and 14.

Other types of steel meeting the requirements of ASTM A514 rely more heavily on alloying elements to assure the hardenability requirement. With greater alloy content, the quenching rate can be less severe.

In the primary hot rolling of plate, inclusions will be elongated and rolled out in the direction of rolling, that is, parallel to the plate surface. The morphology of these rolled-out inclusions will not be affected by the subsequent quench and tempering operations.

High Cycle Fatigue Crack

The beam tested was a welded wide-flange shape. In fabrication, the web and flanges were tack-welded to maintain fit-up while the final fillet welds were made.

Examination of the fracture surface at the fillet welds showed that the fatigue crack started at the end of one of these tack welds. The tack weld had not fused to the web and flange, and produced a defect known as cold lap. (The fillet weld subsequently deposited did not melt through the tack weld.) It was this defect which served to initiate the high cycle fatigue crack. (See Fig. 15.)

The surface of the high cycle fatigue crack was macroscopically fine textured and was normal to the flange and web (Fig. 5).

Microscopic examination of the high cycle fatigue crack on Specimen 7 (Fig. 11) reveals that the crack grows normal to the flange surface independently of any gross microstructural features. There is only a slight tendency to delaminate along rolled-out inclusions or to have a branched fracture path. The etched section shows that the fracture path follows the microstructure boundaries but the overall fracture path seems independent of the microstructural morphology and responsive only to the loading conditions.

Low-Cycle Fatigue Crack

At the extremity of the flange the low-cycle fatigue crack assumes a macroscopically rough surface and is oriented at an angle of approximately 50° to the flange surface.

This oblique fracture surface when examined microscopically shows a strong tendency to delaminate along planes of rolled-out inclusions (Fig. 12). The overall direction of the fracture is independent of the microstructural features since the delaminations only influence the fracture surface in the local region of the defects. Otherwise the fracture direction is independent of microstructure and seems responsive primarily to the loading and stress conditions.

Web and Flange Crack Ends

The ends of the flange and web cracks were polished parallel to their planes as shown in Fig. 4. The web crack was approximately 20° to the web surface. The flange crack was approximately 60° to the flange surface. Polished sections (Figs. 13 and 14) reveal that the nature of the cracks are quite different.

The web crack is wide and blunt with a discontinuous step to a finer size near the tip (Fig. 13). This latter portion of the crack may have been caused by the impact loading when the

flange crack broke through one end of the flange and rapidly transferred load to the web.

The etched web crack specimen showed no strong relationship between crack direction and microstructure. There is little tendency for the crack to branch.

The polished flange crack end shows (Fig. 14) that the fracture is very fine and generally follows a path through inclusions and carbides which were formed during tempering. There is multiple branching of the crack tip along its path. On a very fine scale (Fig. 14-arrow) the crack follows a path along microstructure boundaries between carbides and inclusions. The lower figure is of such a magnification that its field can not be seen in the upper one.

5. CONCLUSIONS AND RECOMMENDATIONS

The purpose of this study was to investigate the fatigue behavior of a welded beam with an initial crack in the last phase of its fatigue life and to record crack propagation and stress redistribution. The beam was welded of A514 steel fabricated from flame cut plates. It had been tested in high-cycle fatigue, and the low-cycle fatigue test was actually an additional phase of the overall test. The following conclusions and recommendations were reached:

1. The stress distribution corresponding to the crack growth was recorded after each 5000 cycles by electrical strain gages and a digital strain indicator for static load. The continuous recording of strains during cycling was tried using strain gages and a Brush Recorder, but the results were not suitable for the purposes of the study. For more accurate observation the number of strain gages should be increased.
2. The fracture surface study reveals a transition from smooth to rough texture as the crack grows from initial size to final beam failure. The initial fracture is normal to the applied stress while the final fracture is inclined to the applied stress.

3. The fracture path follows inclusions, carbides and microstructure boundaries. The microstructure is sufficiently fine so that its effect is minor and the overall fracture path is responsive primarily to loading conditions.

4. There is a very slight tendency during the first phase of fracture propagation to delaminate along rolled-out inclusions. A greater delamination tendency is observed during the second phase of fracture growth.

5. The crack initiated at a tack weld end and grew very slowly through the flange-to-web welds, the central part of the flange, and the top of the web. During the last phase of the fatigue life (the "low-cycle fatigue test") the observed fracture surface transition apparently is correlated to a very significant stress redistribution and to the increasing size of the yield stress zone at the crack tip.

6. After the stress range was decreased it was observed that the crack propagation rate was higher than expected from theoretical predictions and the rate came closer to the theoretical values only after propagation.

7. The visual observation by microscope using a net of reference lines may be the simplest way of recording crack propagation with sufficient accuracy. For very small cracks the observation of the crack tip during cycling may be recommended for better

recognition of the actual crack end. Additional crack propagation gages may be used to confirm the results.

8. The theoretical analysis of three-ended cracks propagation in a beam is to be developed.

6. NOMENCLATURE

L_1, L_2	load (kips)
N	number of cycles
2a	crack length
w	flange width
σ_{ys}	yield stress
k	stress intensity factor
$2r_y$	zone of plasticity

7. ACKNOWLEDGEMENTS

This paper presents the results and discussion of an experimental pilot study of the fatigue of a beam with a crack. The investigation is one phase of a major research program designed to provide information on the behavior and design of joined structure under low-cycle fatigue.

The investigation was conducted at Fritz Engineering Laboratory, the Department of Civil Engineering, and the Department of Metallurgy and Materials Science, Lehigh University, Bethlehem, Pennsylvania. The Office of Naval Research, Department of Defense, sponsored the research under contract N 00014 -68 - A-514; NR 064-509. The program manager for the overall research project is Lambert Tall.

The guidance of, and the suggestions from, the members of the special Advisory Committee on Low-Cycle Fatigue is gratefully acknowledged. The authors are indebted to Robert D. Stout for his helpful comments.

The authors express their thanks to their co-workers Manfred Hirt and Salvador Lozano for help with the testing and to Kenneth Harpel, laboratory foreman, and his staff, for their assistance during testing. Sincere thanks are due to Miss Joanne Mies

who typed the report and to Jack M. Gera and Mrs. Sharon Balogh who prepared the drawings.

Lynn S. Beedle is Director of Fritz Engineering Laboratory; David A. Van Horn is Chairman of the Department of Civil Engineering; George P. Conard II is Chairman of the Department of Metallurgy and Materials Science; and Joseph F. Libsch is Vice President for Research, Lehigh University.

8. TABLES AND FIGURES

TABLE 1
Crack Propagation Rate Versus $\frac{2a}{w}$

2a (in.)	$\frac{2a}{w}$	stress range (ksi)	ΔK (ksi in)	$\frac{d(2a)}{dN}$ (in/cycle)
0.2	0.0294	42	23.5	4.4×10^{-6}
0.5	0.0733	42	37.4	1.8×10^{-5}
1.0	0.147	42	53.5	3.6×10^{-5}
1.55	0.227	42	68	6×10^{-5}
1.55	0.227	22.6	36.4	1.7×10^{-5}
2.0	0.294	22.6	43	2.6×10^{-5}
2.5	0.366	22.6	49	4×10^{-5}
3.5	0.513	22.6	64.5	6×10^{-5}
4.0	0.586	22.6	75	8×10^{-5}
6.5	0.660	22.6	88	1.2×10^{-4}
5.0	0.735	22.6	108	2×10^{-4}

(2a) - crack length

w - width of the flange

BEAM PWC 152

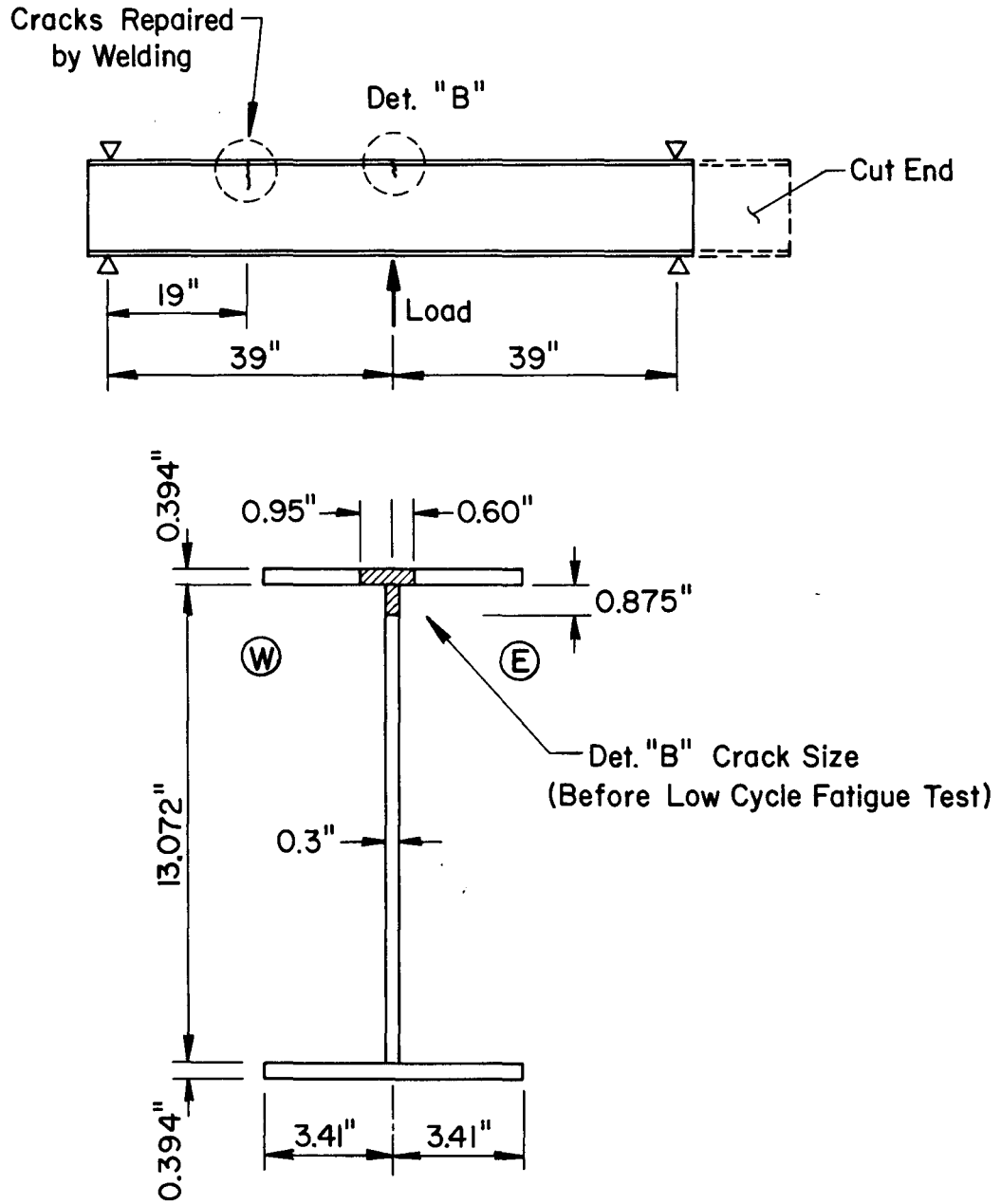


Fig. 1 Beam PWC152.

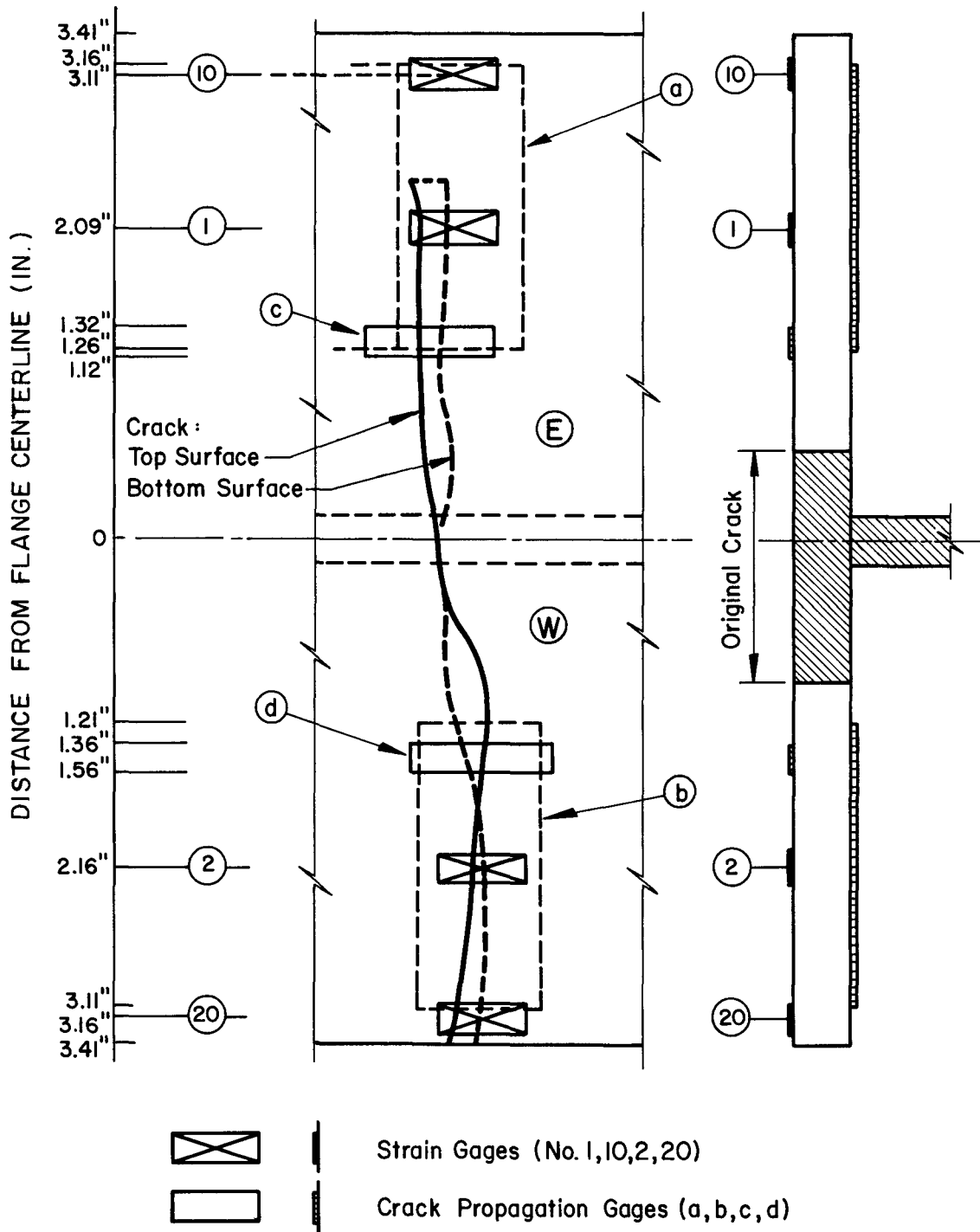


Fig. 2 Shape of the Crack and the Position of Strain Gages in the Flange.

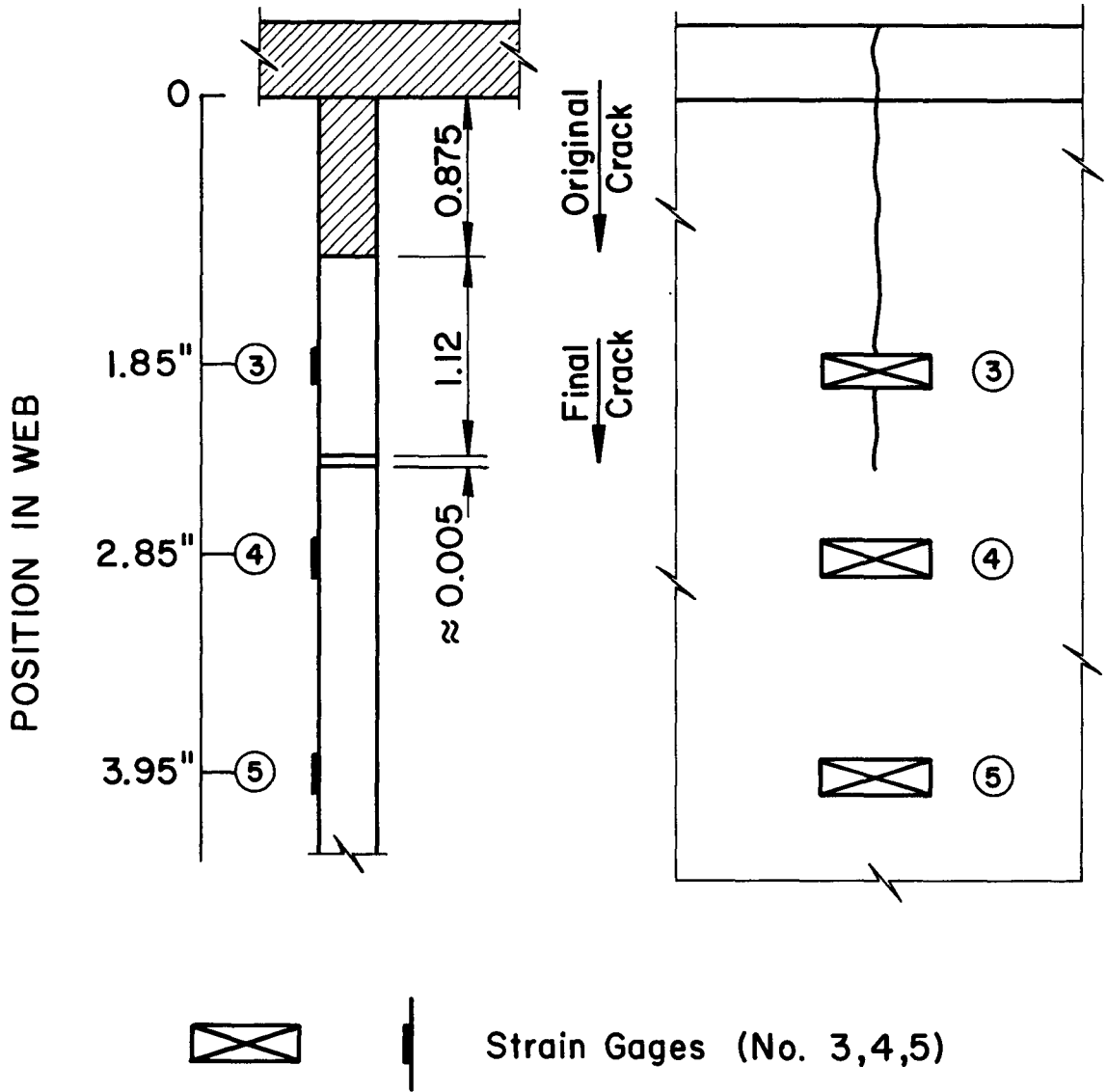


Fig. 3 Crack in the Web and Position of the Strain Gages.

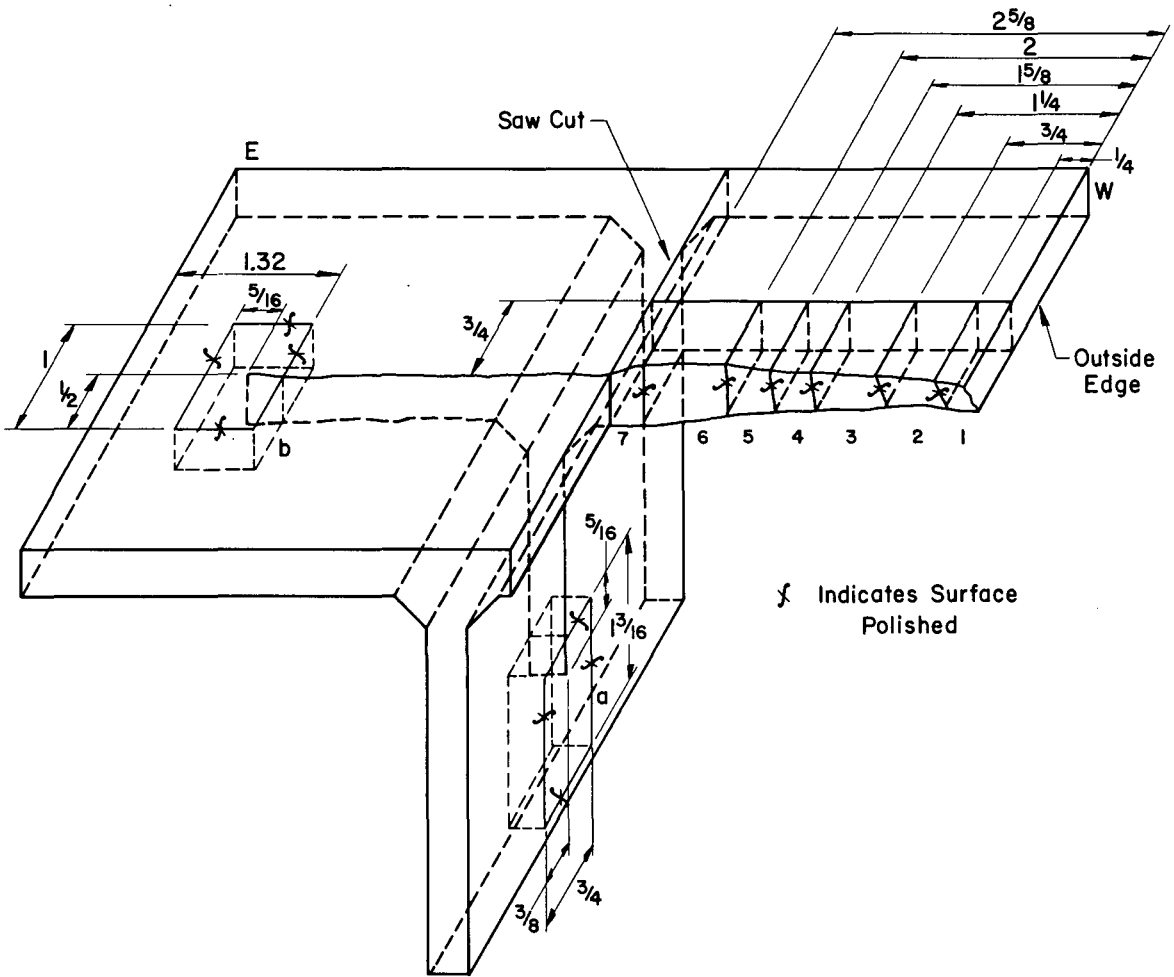
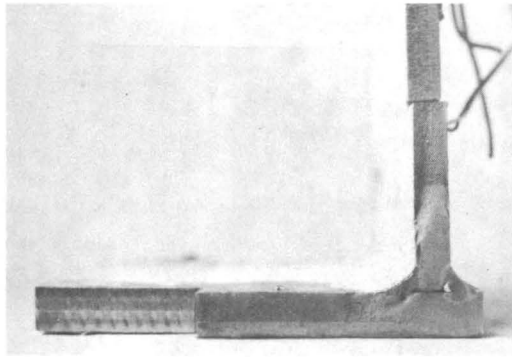
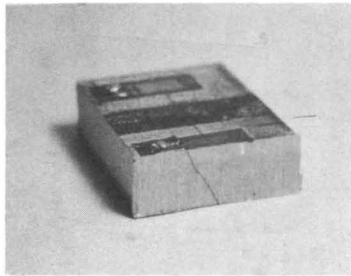


Fig. 4 Sectioning of the Beam for Metallurgical Investigation.

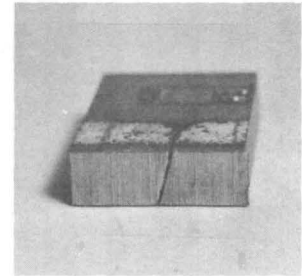
358.4



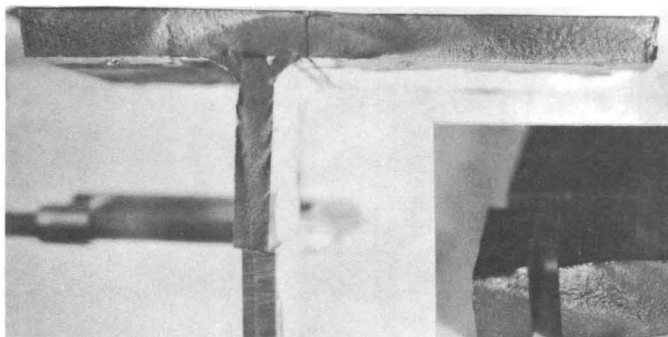
End of Flange Crack



End of Flange Crack



End of Web Crack



Flange W

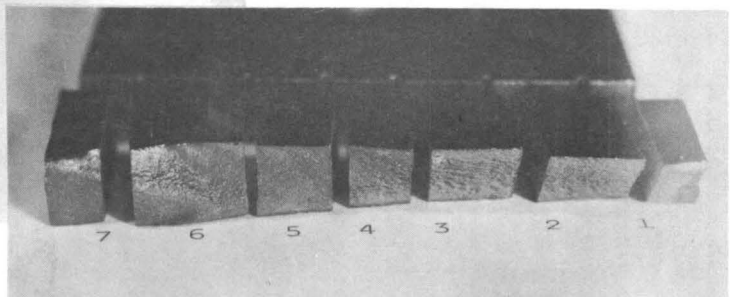


Fig. 5 Metallurgical Specimens

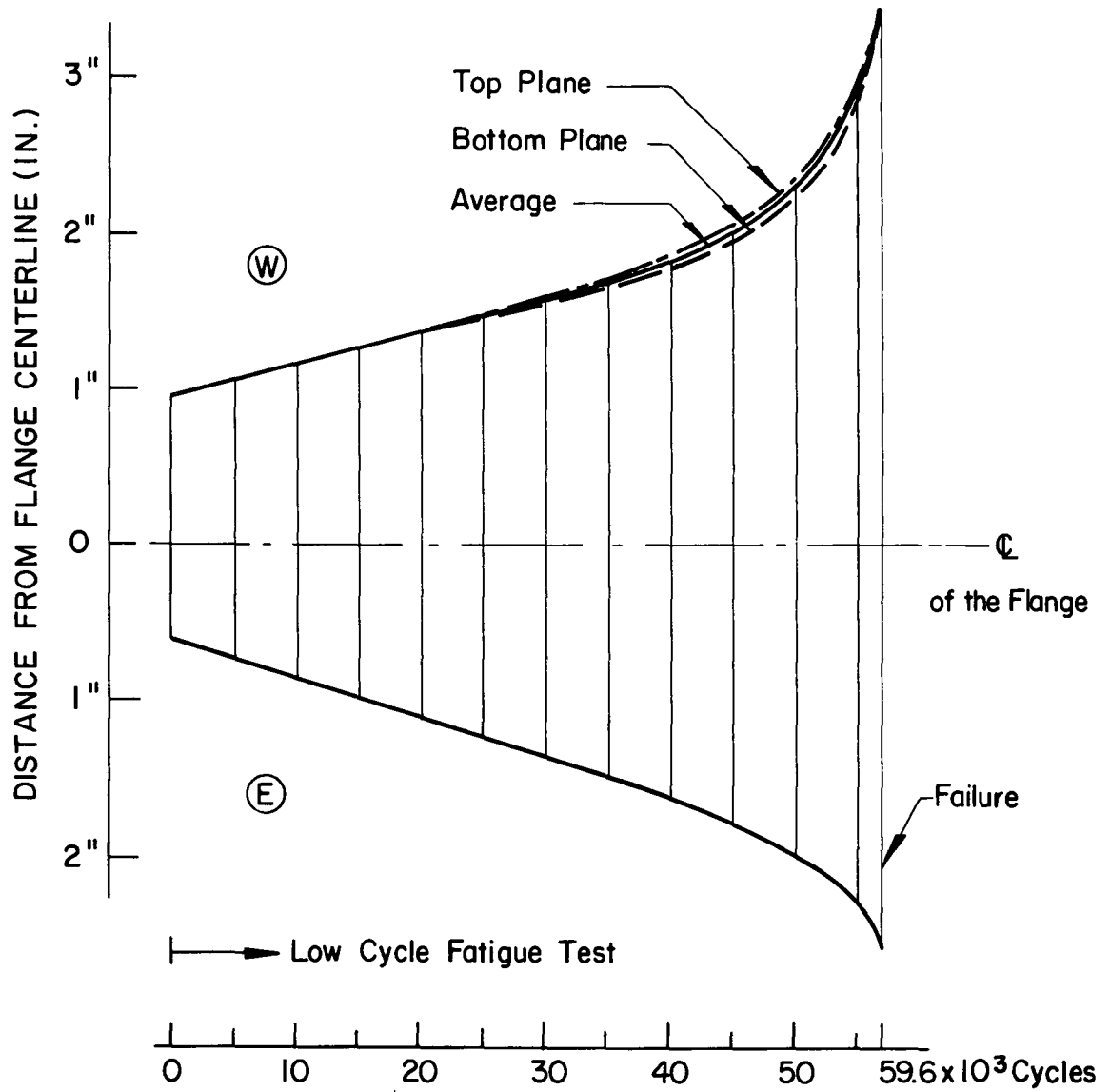


Fig. 6 Crack Length Versus Number of Cycles.

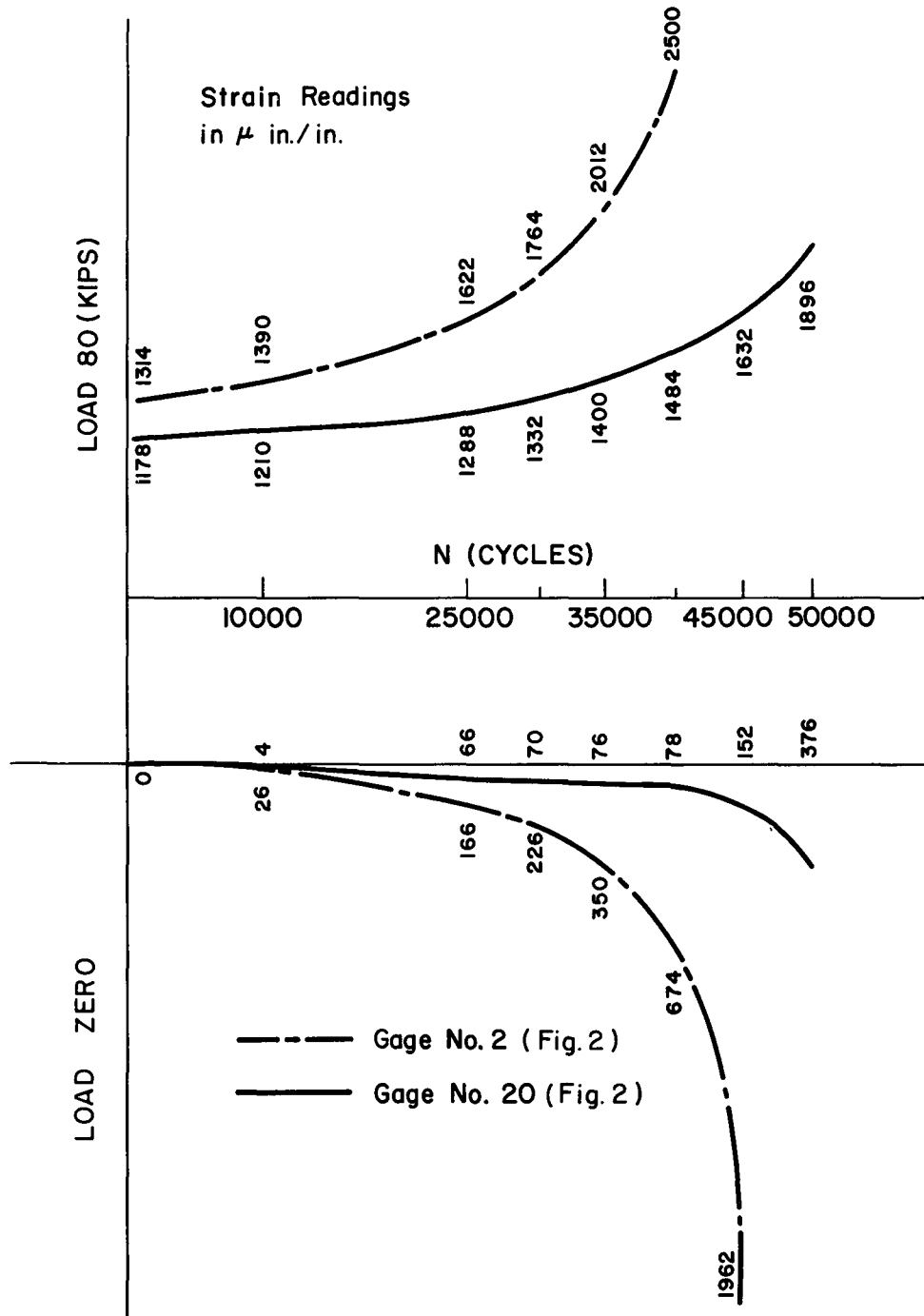


Fig. 7 Strain Readings (Gages 2, 20).

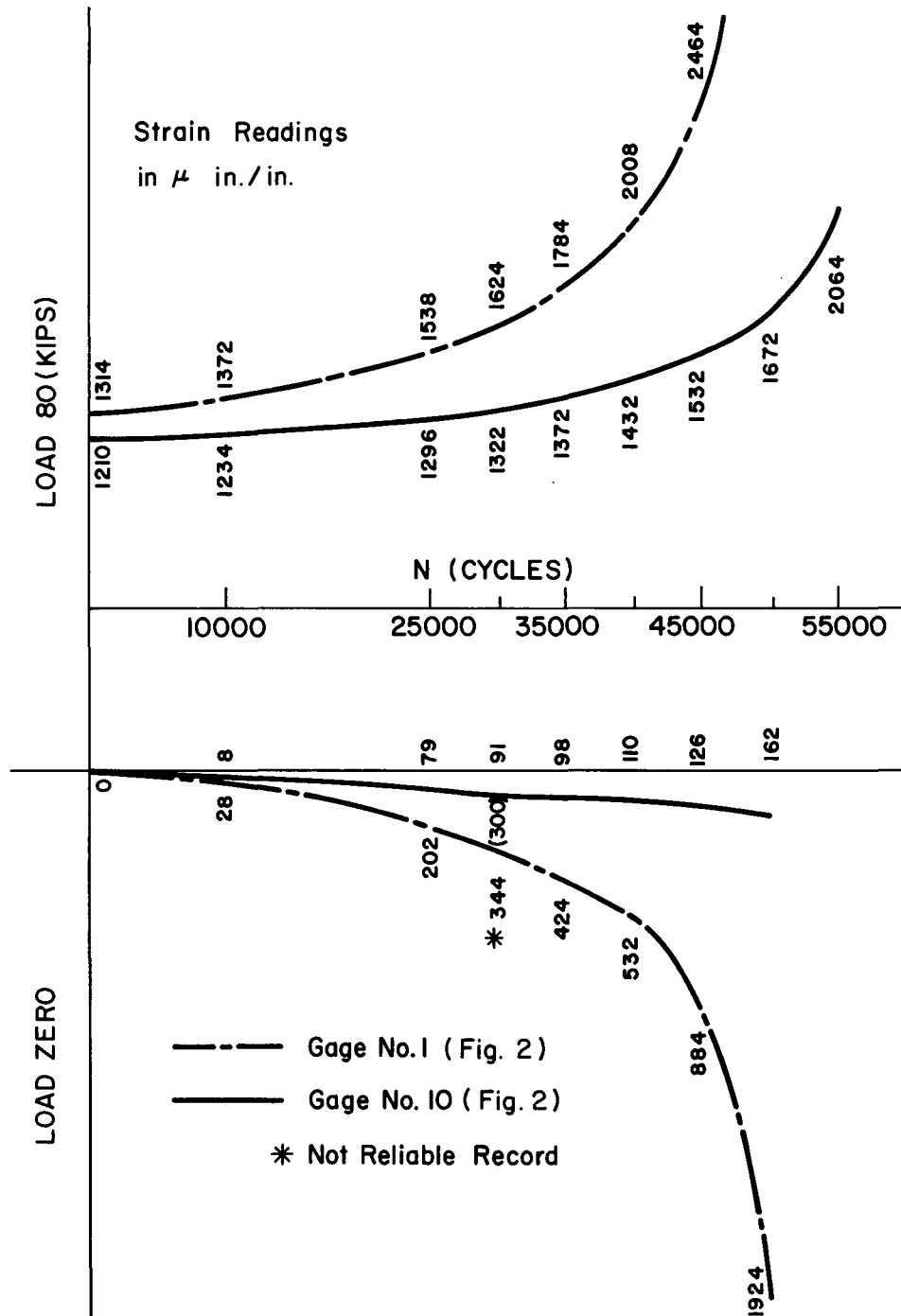


Fig. 8 Strain Readings (Gages 1, 10).

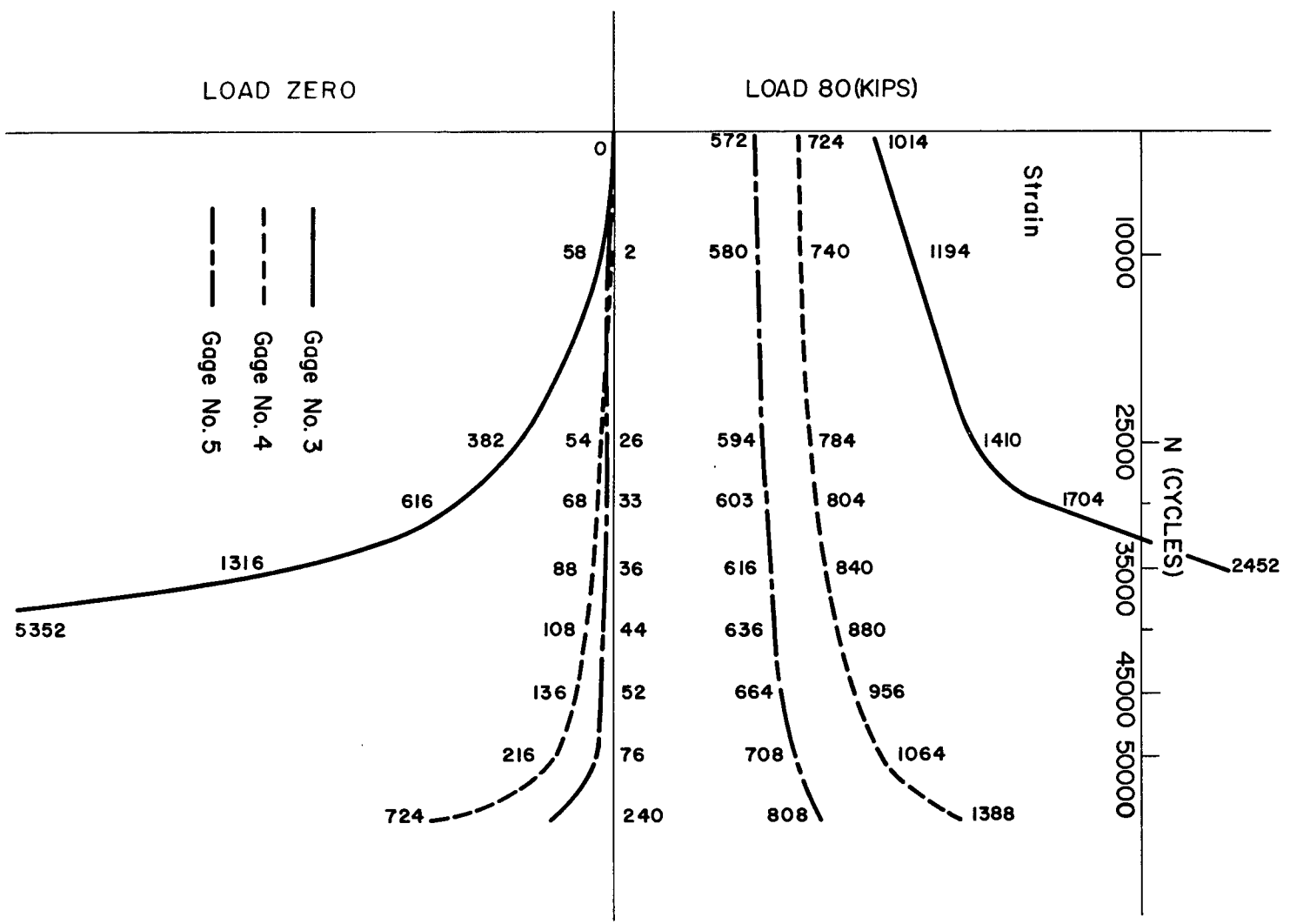


Fig. 9 Strain Readings (Gages 3, 4, 5).

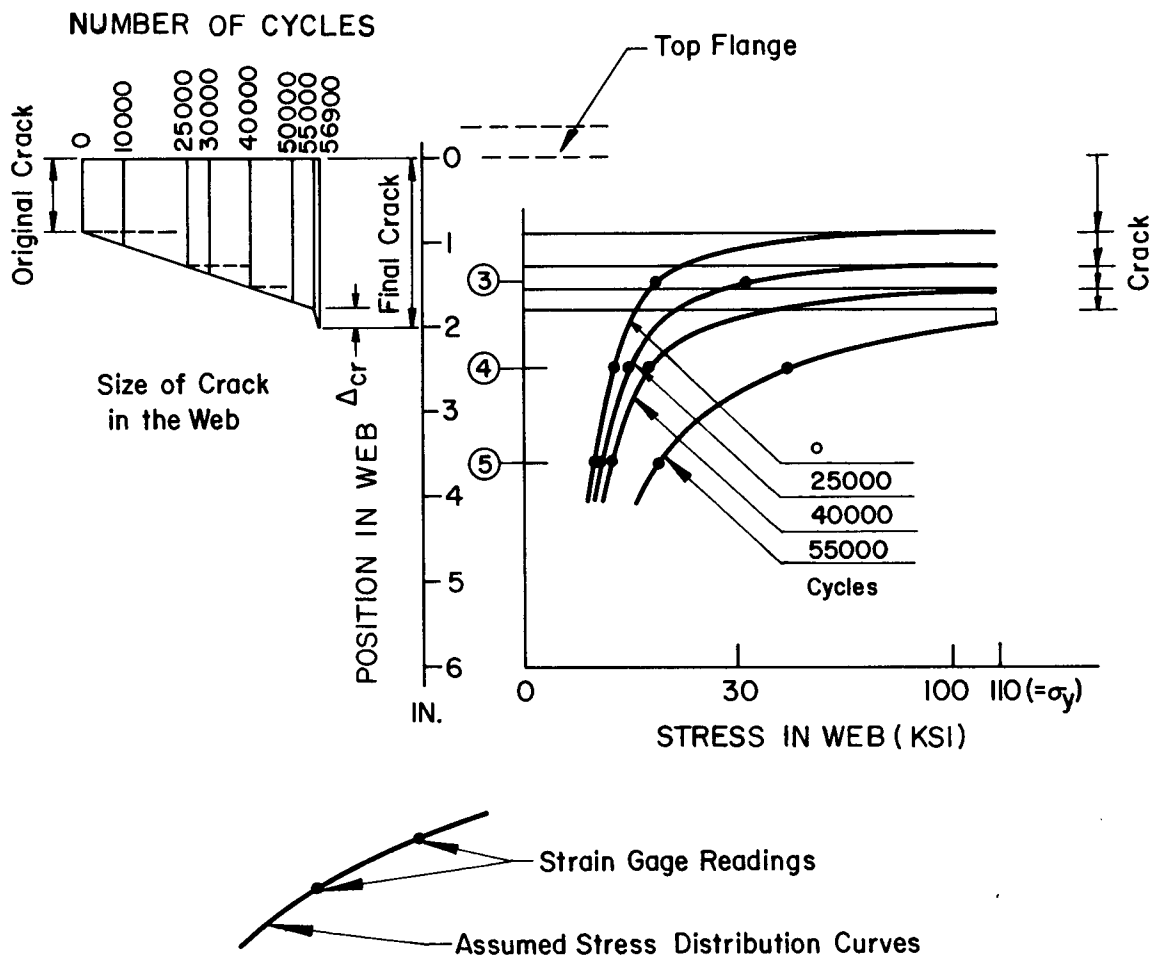
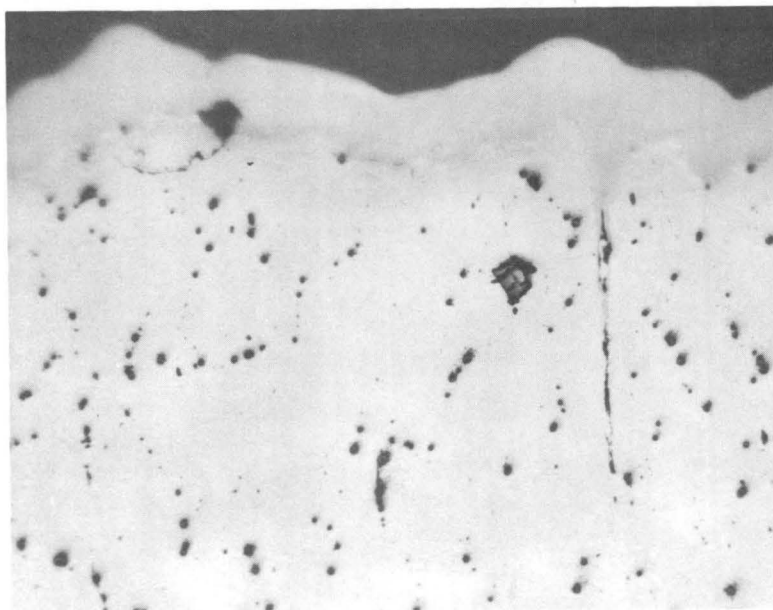


Fig. 10 Crack Propagation and Stress Redistribution in the Web.



▲ Rolling
▼ Direction

Carbides and Inclusions Visible.

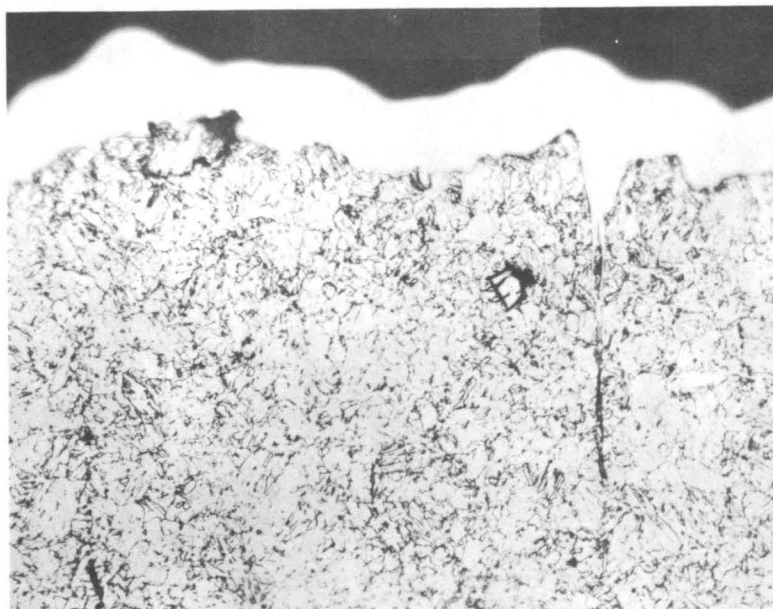
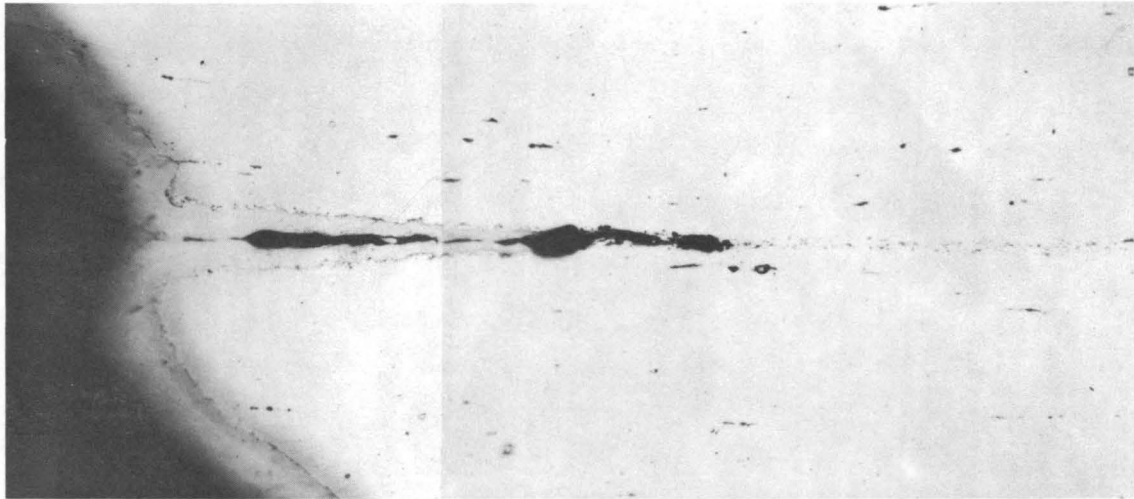


Fig. 11 Specimen 7. Above-Unetched, Below-Nital Etch (250x).

358.4



←→ Rolling Direction

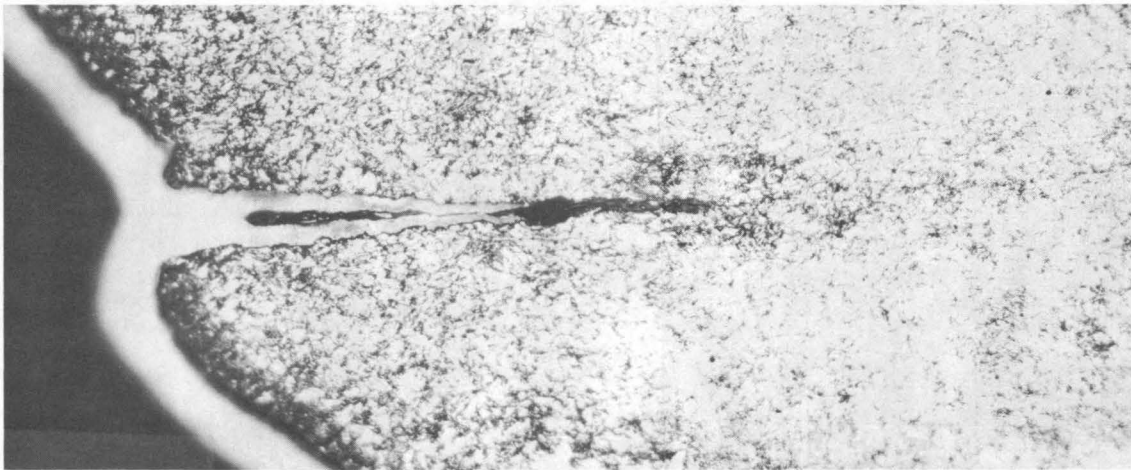
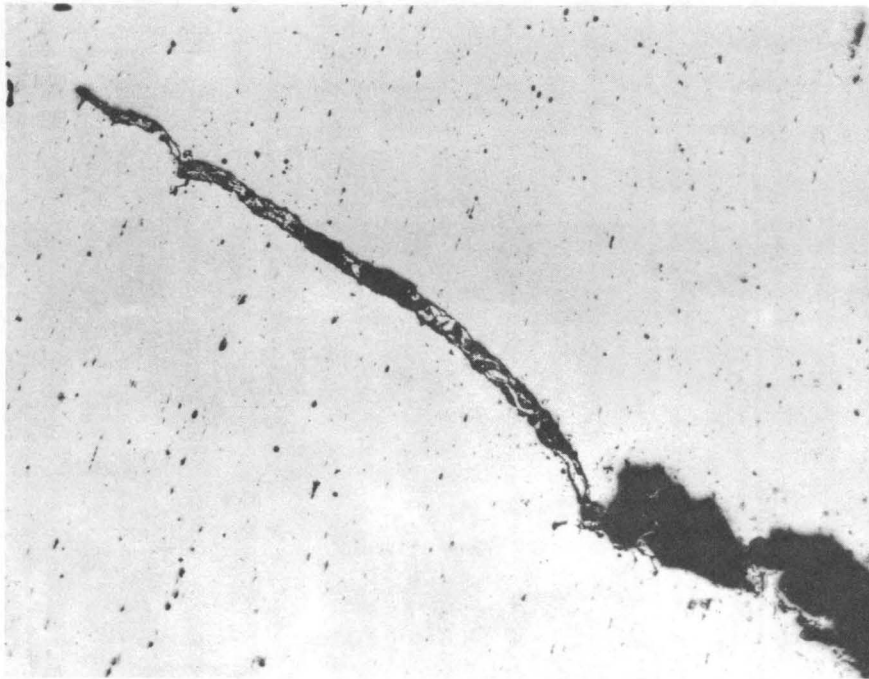
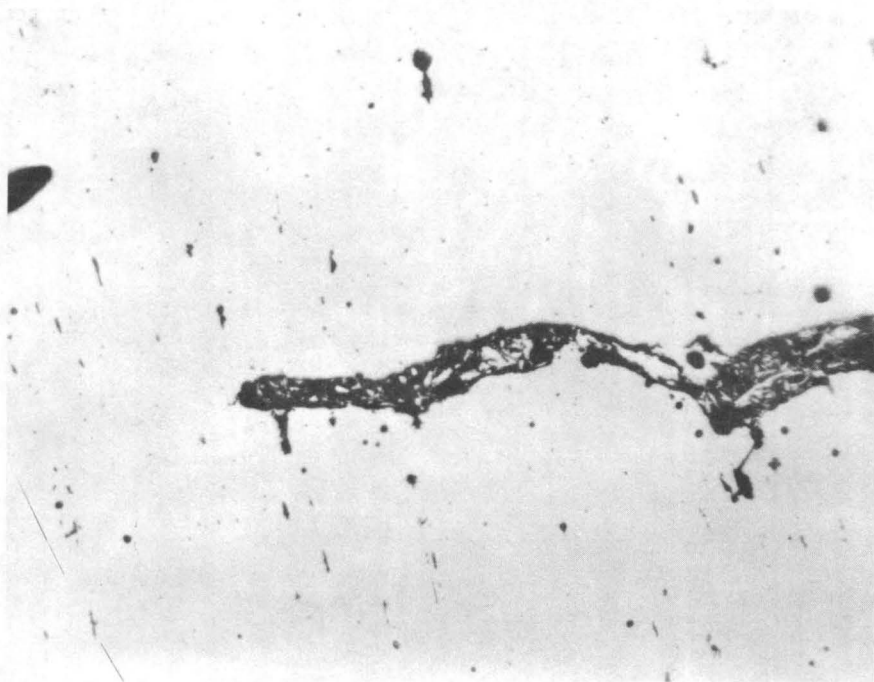


Fig. 12 Specimen 2. Above-Unetched, Below-Nital Etch (250x).

358.4



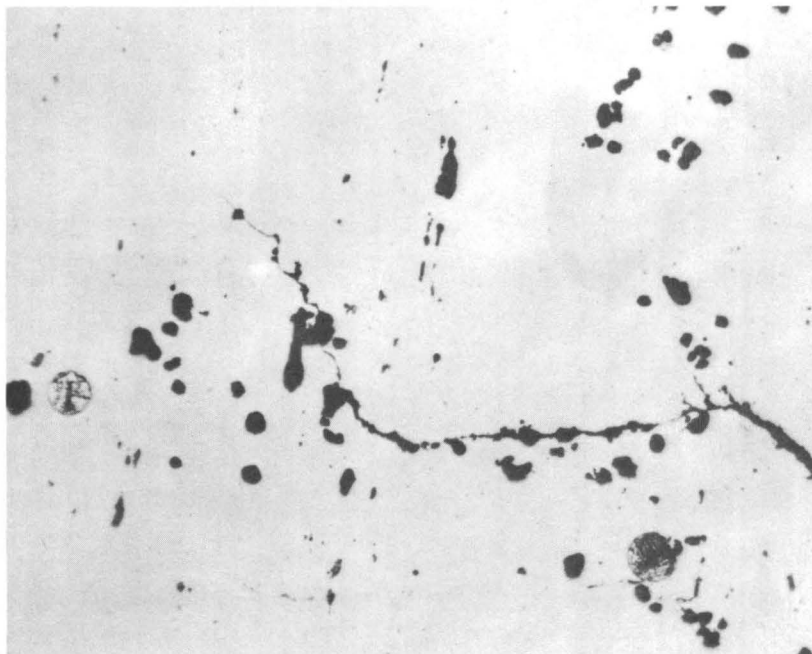
75x



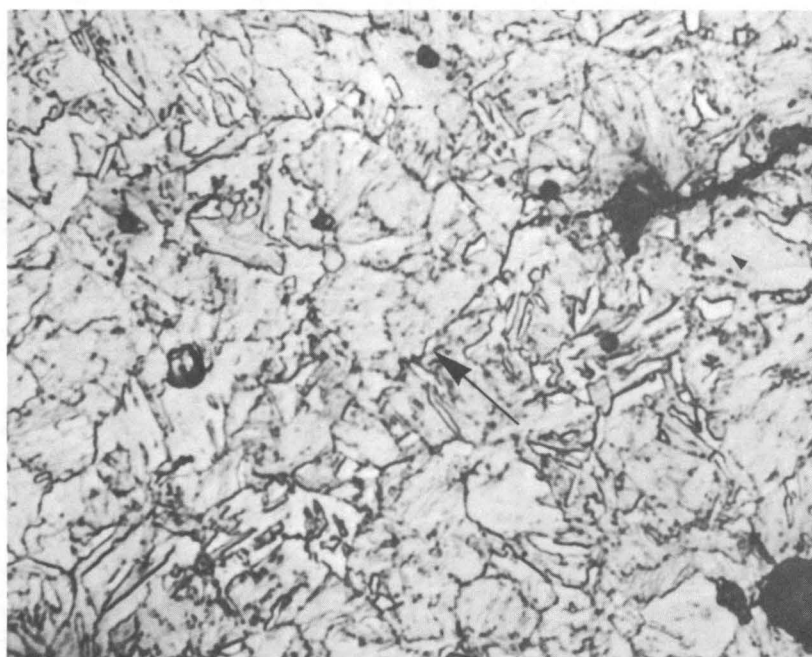
250x

Fig. 13 End of Crack Polished in Plane of Web.

358.4



250x (Unetched)



1000x (Nital Etch-Crack Indicated by Arrow,
Field Not Visible in Photo Above).

Fig. 14 End of Flange Crack. Polished Parallel
to Outside Surface of Flange.

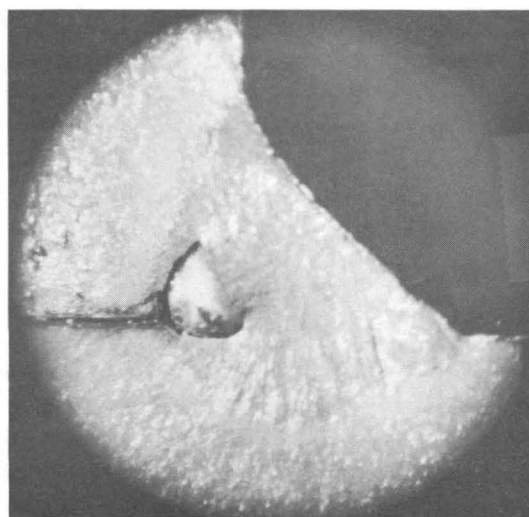
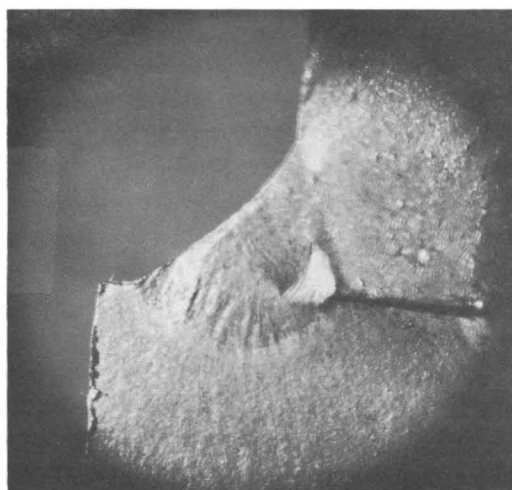
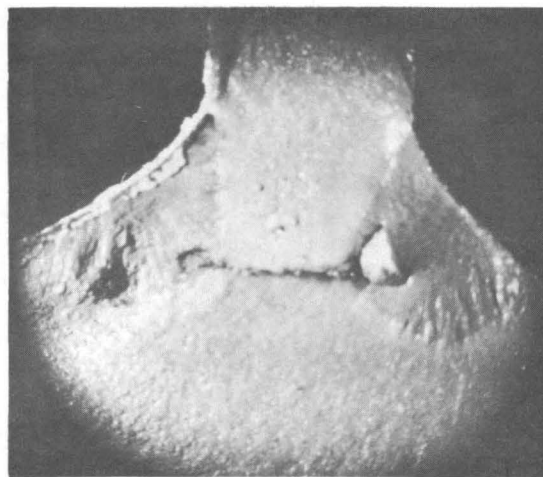
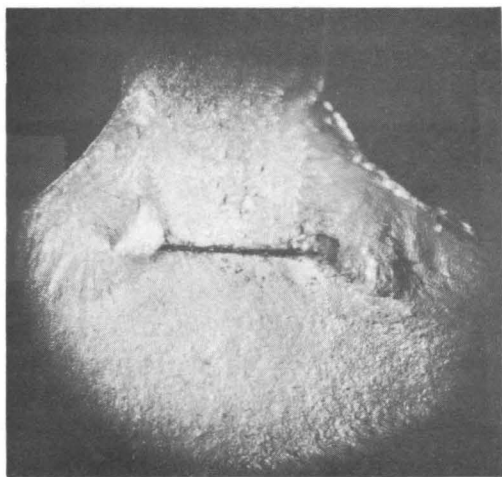


Fig. 15 Macrophotographs of Web-to-Flange Fillet Welds
in Fracture Surface.

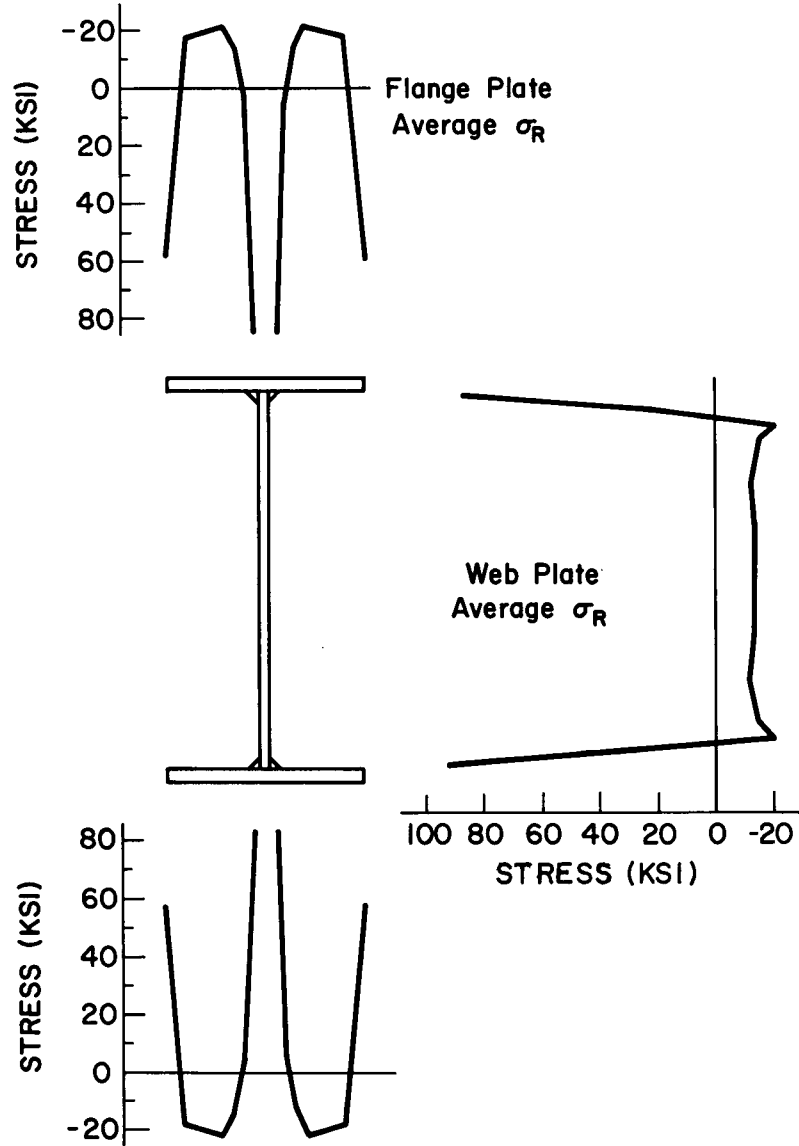


Fig. 16 Residual Stress in PWC152 Beam.

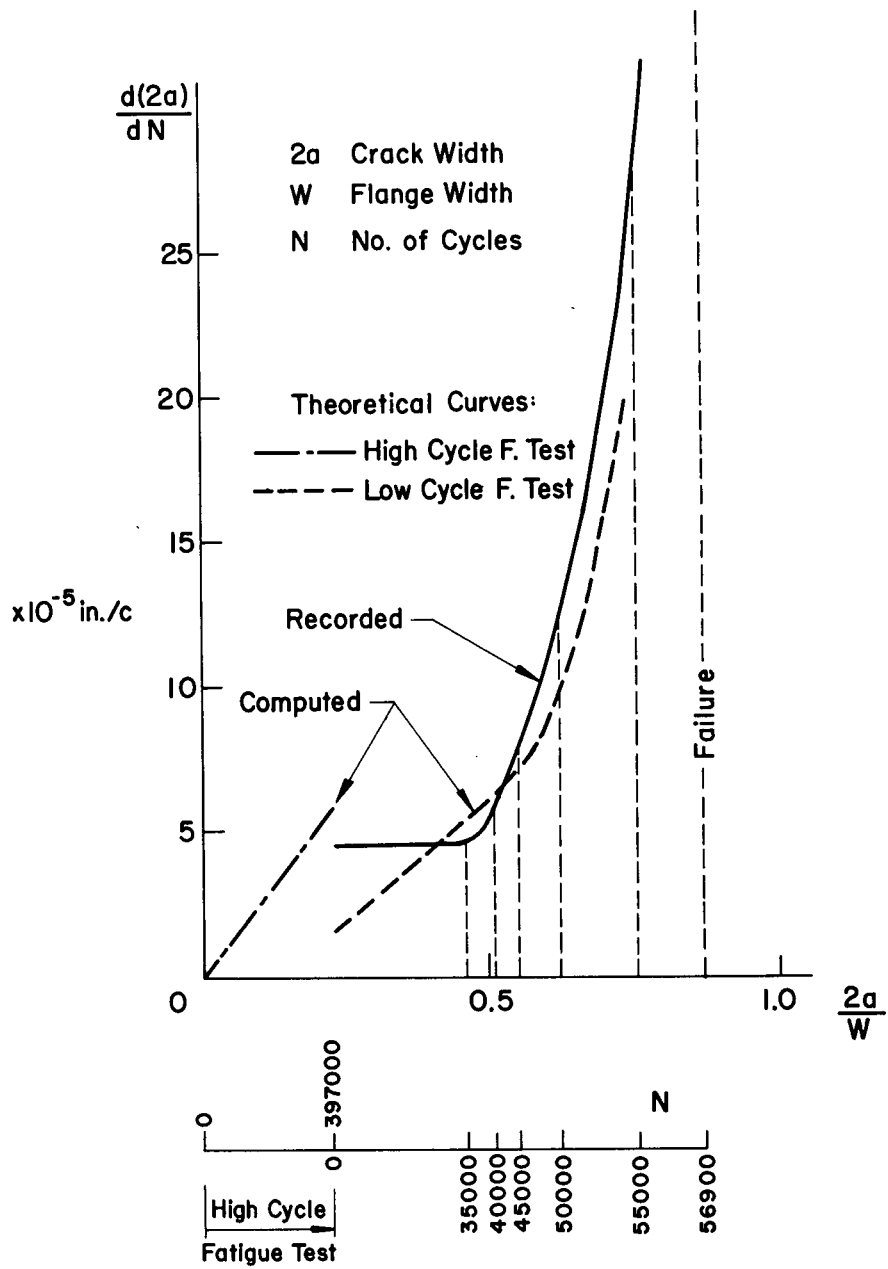


Fig. 17 Crack Propagation Rate Versus Position in the Flange.

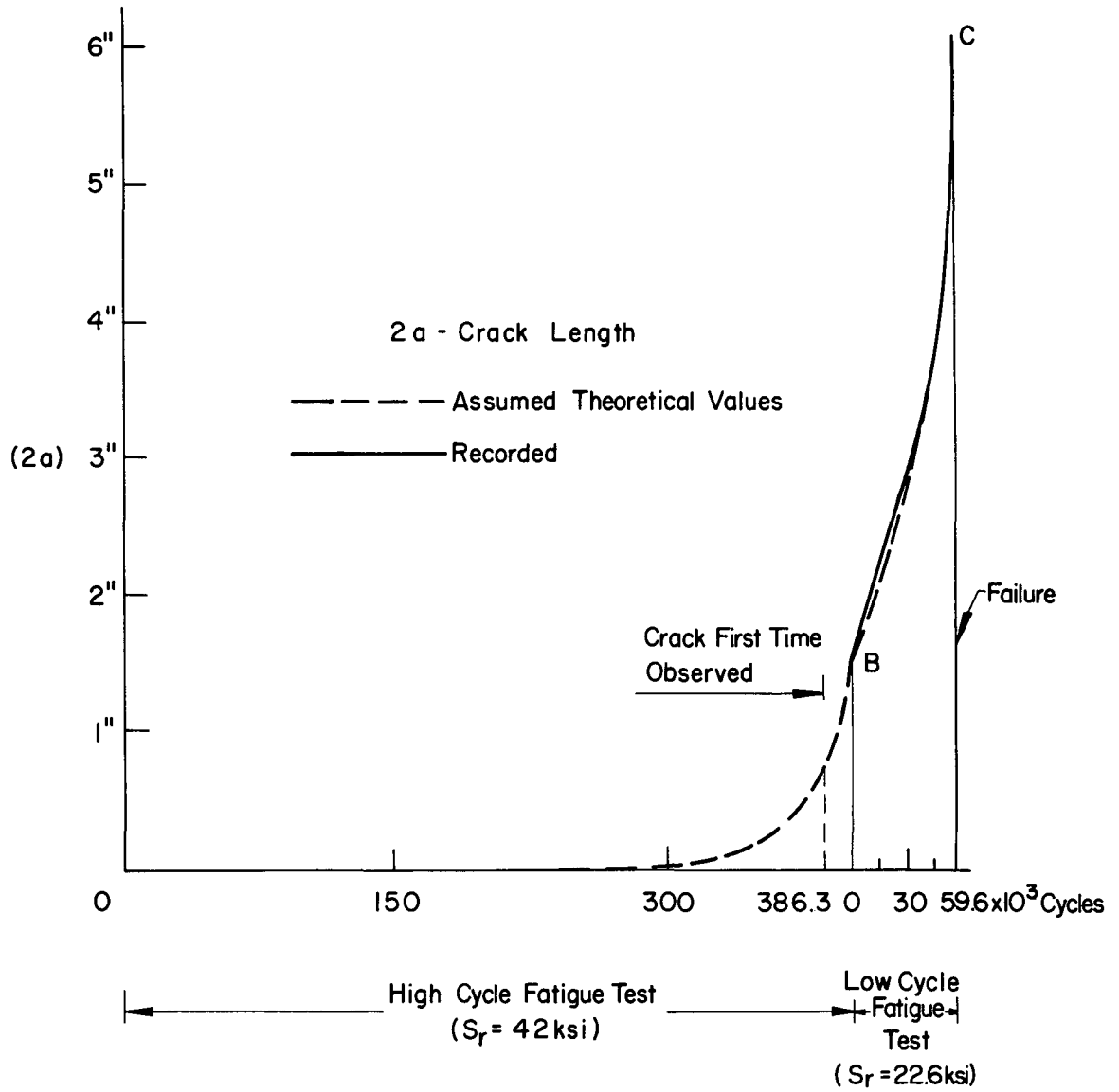


Fig. 18 Crack Length Versus Number of Cycles.

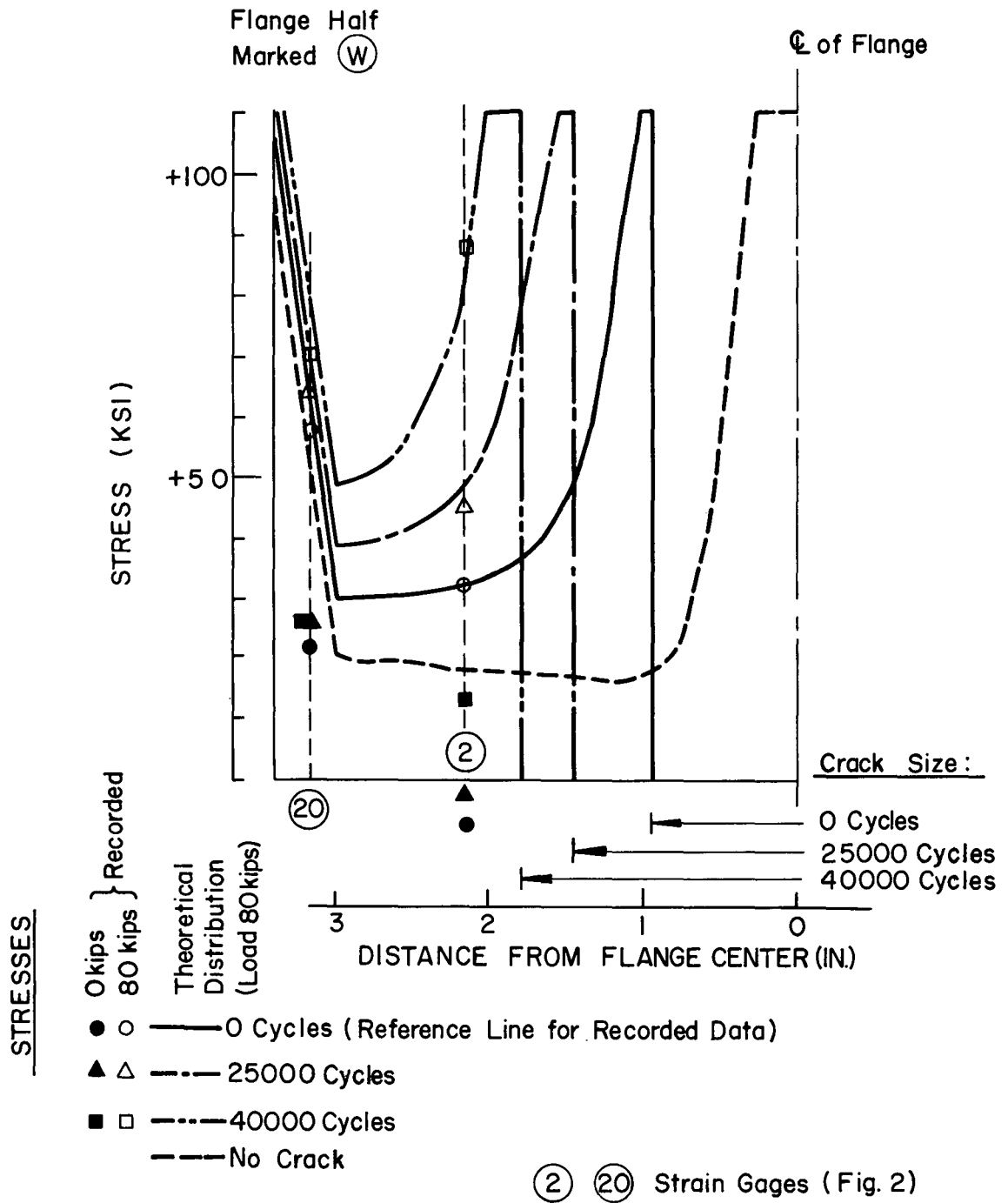


Fig. 19 Stress Redistribution in Flange With Crack.

9. REFERENCES

1. M. A. Hirt, B. T. Yen, J. W. Fisher
FATIGUE STRENGTH OF ROLLED AND WELDED BEAMS,
Fritz Eng. Laboratory Report 334.2 (in prepara-
tion) Lehigh University
2. S. Lozano, P. Marek
RESIDUAL STRESS IN BEAM, Fritz Eng. Laboratory
Report 358.5 (in preparation) Lehigh University
3. H. Nordberg, R. W. Hertzberg
FATIGUE CRACK PROPAGATION IN A514 STEEL, Fritz
Eng. Laboratory Report 358.7, Lehigh University
4. R. J. Smith, P. Marek, and B. T. Yen
STRESS DISTRIBUTION IN PLATE WITH CRACK, Fritz
Eng. Laboratory Report 358.8 (in preparation)
Lehigh University
5. American Society for Testing and Materials
STANDARD SPECIFICATION FOR HIGH-YIELD STRENGTH,
QUENCHED AND TEMPERED ALLOY STEEL PLATE, SUITABLE
FOR WELDING, 1967

DOCUMENT CONTROL DATA - R & D

(Security classification of title, body of abstract and indexing annotation must be entered when the overall report is classified)

1. ORIGINATING ACTIVITY (Corporate author)		2a. REPORT SECURITY CLASSIFICATION	
		2b. GROUP	
3. REPORT TITLE CRACKED BEAM TEST			
4. DESCRIPTIVE NOTES (Type of report and inclusive dates)			
5. AUTHOR(S) (First name, middle initial, last name) P. Marek, M. Perlman, A. W. Pense, L. Tall			
6. REPORT DATE May 1969	7a. TOTAL NO. OF PAGES 46	7b. NO. OF REFS 5	
8a. CONTRACT OR GRANT NO. N 00014-68-A-514;NR 064-509	9a. ORIGINATOR'S REPORT NUMBER(S) 358.4		
b. PROJECT NO. 358	9b. OTHER REPORT NO(S) (Any other numbers that may be assigned this report)		
c.			
d.			
10. DISTRIBUTION STATEMENT			
11. SUPPLEMENTARY NOTES		12. SPONSORING MILITARY ACTIVITY	

13. ABSTRACT

This report presents the results of and discussion on an experimental investigation of a welded beam with a crack tested in the low-cycle fatigue range.

In the investigation, an attempt was made to develop techniques for evaluating low-cycle tests. The tests conducted were designed for different kinds of measurements for beam tests, to gain experience with data recording, to obtain preliminary information about crack propagation, to try to record stress redistribution, and to obtain information on the metallurgical structure sensitivity of low-cycle and high-cycle fatigue tests.

The test was conducted on a beam already cracked in a high-cycle fatigue test. The relationship between the crack propagation rate, stress redistribution and the texture of the crack surface were observed. The recorded data were compared with available theoretical or experimental results.